



Pauli-Heisenberg Oscillations in Electron Quantum Transport

Karl Thibault,^{1,*} Julien Gabelli,^{2,†} Christian Lupien,^{1,‡} and Bertrand Reulet^{1,2,§}

¹*Département de physique, Université de Sherbrooke, Sherbrooke, Québec J1K 2R1, Canada*

²*Laboratoire de Physique des Solides, Université Paris-Sud, CNRS, UMR 8502, F-91405 Orsay Cedex, France*

(Received 4 November 2014; revised manuscript received 18 March 2015; published 11 June 2015)

We measure the current fluctuations emitted by a normal-metal–insulator–normal-metal tunnel junction with a very wide bandwidth, from 0.3 to 13 GHz, down to very low temperature $T = 35$ mK. This allows us to perform the spectroscopy (i.e., measure the frequency dependence) of thermal noise (no dc bias, variable temperature) and shot noise (low temperature, variable dc voltage bias). Because of the very wide bandwidth of our measurement, we deduce the current-current correlator in the time domain. We observe the thermal decay of this correlator as well as its oscillations with a period h/eV , a direct consequence of the effect of the Pauli and Heisenberg principles in quantum electron transport.

DOI: 10.1103/PhysRevLett.114.236604

PACS numbers: 72.70.+m, 73.23.-b

Introduction.—Conduction of electrons in matter is ultimately described by quantum mechanics. Yet at low frequency or long time scales, low-temperature quantum transport is perfectly described by this very simple idea: electrons are emitted by the contacts into the sample which they may cross with a finite probability [1,2]. Combined with Fermi statistics, this partition of the electron flow accounts for the full statistics of electron transport [3]. When it comes to short time scales, a key question must be clarified: are there correlations between successive attempts of the electrons to cross the sample? While there are theoretical predictions [1] and several experimental indications for the existence of such correlations [4–6], no direct experimental evidence has ever been provided.

In order to probe temporal correlations between electrons, we have studied the correlator between current fluctuations $i(t)$ generated by the sample measured at two times separated by t , $C(t) = \langle i(t')i(t'+t) \rangle$, where $\langle \cdot \rangle$ denotes statistical averaging. We calculate this correlator by a Fourier transform of the detected frequency-dependent power spectrum of current fluctuations generated by a tunnel junction placed at very low temperature. The very short time resolution required to access time scales relevant to electron transport is achieved from the ultrawide bandwidth, 0.3–13 GHz, of our detection setup.

In this Letter, we report the measurement of the frequency-dependent noise spectral density of both thermal noise (no dc bias, various temperatures) and shot noise (lowest temperature, various voltage biases), from which we determine the current-current correlator in time domain $C(t)$. These observations provide direct experimental proof of how temperature and voltage bias control the electron flow: while temperature T leads to a jitter which tends to decorrelate electron transport after a time $\hbar/k_B T$, the bias voltage V induces strong correlations or anticorrelations which oscillate with a period h/eV . This oscillation is a direct consequence of the Pauli and Heisenberg principles.

Our experiment reveals how time scales related to voltage and temperature operate on quantum transport in a simple coherent conductor. In complex quantum systems, the method we have developed might offer direct access to other relevant time scales related, for example, to internal dynamics, coupling to other degrees of freedom, or correlations between electrons.

Principle of the experiment.—The measurement has been performed on a $10 \mu\text{m} \times 1 \mu\text{m}$ Al/Al oxide/Al tunnel junction fabricated by photolithography using the Dolan bridge technique [7]. The junction is placed on the cold plate of a dilution refrigerator, whose temperature can be adjusted above its base value, 8 mK, with a resistive heater. An ~ 500 G perpendicular magnetic field keeps the Al in its nonsuperconducting state, with negligible effect on charge transport. The resistance of the junction $R = 51 \Omega$ is voltage and temperature independent within less than 1% in all measurements. The detection setup we have used is similar to that of Ref. [8] and depicted in Fig. 1. The junction is dc biased through the dc port of a bias tee after cryogenic low-pass filtering. The high-frequency current fluctuations generated by the junction are transmitted through a superconducting coaxial cable to a high-electron-mobility transistor 0.3–13 GHz amplifier placed at 3 K. The resulting signal is further amplified at room temperature and down-converted using a frequency mixer to low frequency by multiplication with a local oscillator of variable frequency f , then bandpass filtered between 0.1 and 50 MHz. Using a power detector, we measure the power of that signal which is given by

$$P(f) = \int_{f-\Delta f/2}^{f+\Delta f/2} G_A(f') [S(f') + S_A(f')] df', \quad (1)$$

where $G_A(f)$ is the total gain of the measurement system, $S_A(f)$ the noise added by the detection chain, and $S(f)$ the noise emitted by the sample. Since the measurement's

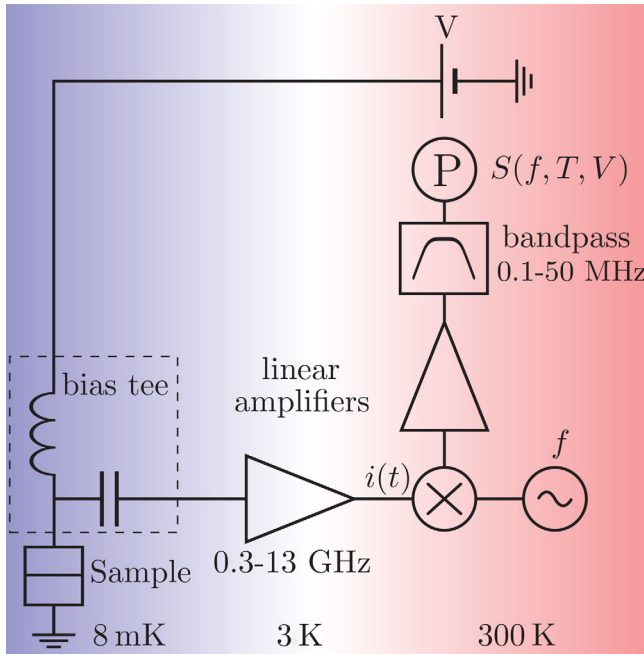


FIG. 1 (color online). Experimental setup. The symbols \otimes and \oplus represent, respectively, a frequency mixer and a power meter.

bandwidth $\Delta f \approx 100$ MHz is much smaller than all relevant frequency scales for electron transport, $S(f)$ is approximately frequency independent within Δf , so Eq. (1) reduces to $P(f) \approx \overline{G}_A(f)[S(f) + \overline{S}_A(f)]\Delta f$. Here, $\overline{G}_A(f)\Delta f = \int G_A(f')df'$ is the mean total gain. It contains the effects of amplification, cable attenuation and imperfections, and the frequency-dependent coupling between the sample and the microwave circuit. $\overline{S}_A(f) = [\overline{G}_A(f)\Delta f]^{-1} \int G_A(f')S_A(f')df'$ is the mean noise added by the detection referred to the sample. It corresponds to a noise temperature varying between ~ 10 K at low frequency and ~ 150 K at high frequency. This increase is mainly due to the coupling between the junction and the microwave circuit that is poor above 10 GHz.

To make an absolute measurement of the noise spectral density $S(f)$, one must calibrate both $\overline{G}_A(f)$ and $\overline{S}_A(f)$ at each frequency. This is achieved by making only one assumption as in Ref. [8], that at high voltage, noise is given by the classical shot noise limit $S(eV \gg hf, k_B T) = eI$ [9,10]. Therefore, for every measurement of $S(f, V, T)$ at any frequency, voltage, or temperature, we measure P vs V at large voltage. From these data, we deduce the values of $\overline{G}_A(f)$ and $\overline{S}_A(f)$. This calibration is repeated for each measurement of $P(f)$, i.e., every ~ 90 s, to cancel out the drift in G_A and S_A .

Results.—The sample's electron temperature is obtained by fitting the measured low-frequency ($hf \ll k_B T$) noise spectral density using $S(f=0, V, T) = GeV \coth(eV/2k_B T)$ [11,12]. We obtain an electron temperature $T = 35$ mK

when the phonon temperature is $T_{\text{ph}} = 8$ mK (measured by a thermometer on the cold plate of the refrigerator). For phonons above 50 mK, we observe $T = T_{\text{ph}}$. We believe the discrepancy between T and T_{ph} at the lowest temperature is due to the emission of noise with very wide bandwidth by the amplifier towards the sample [13]. In the following, the spectral density of noise is expressed in terms of the noise temperature using $T_N(f) = S(f)/(2k_B G)$.

Thermal noise spectroscopy.—In Fig. 2, we show measurements of T_N vs frequency for various electron temperatures T between 35 and 200 mK, when the sample is at equilibrium, i.e., with no bias ($V = 0$). We observe that at low frequency one has $T_N(0) = T$, which is the classical Johnson-Nyquist noise [14,15]. At high frequency $hf \gg k_B T$, all experimental curves approach the zero temperature prediction (dotted black line), which corresponds to the so-called vacuum fluctuations $S_{\text{vac}}(f) = Ghf$. Note that this is a result of our measurement and not a hypothesis. The only assumption made is that the noise at high voltage is given by $S(eV \gg hf, k_B T) = eI$. These quantum zero-point fluctuations had previously been characterized as a function of frequency for a resistor [16] and a superconducting resonator [17].

Whether we measure the variance of the electromagnetic field, including zero-point fluctuations, or only the power emitted by the sample (both differ only by Ghf) cannot be decided here. All one can say is that if the high voltage noise is eI as we suppose, then our results correspond to the prediction of the symmetrized current-current correlator, since we observe the Ghf contribution.

The spectral density of noise at equilibrium is predicted to be [18]

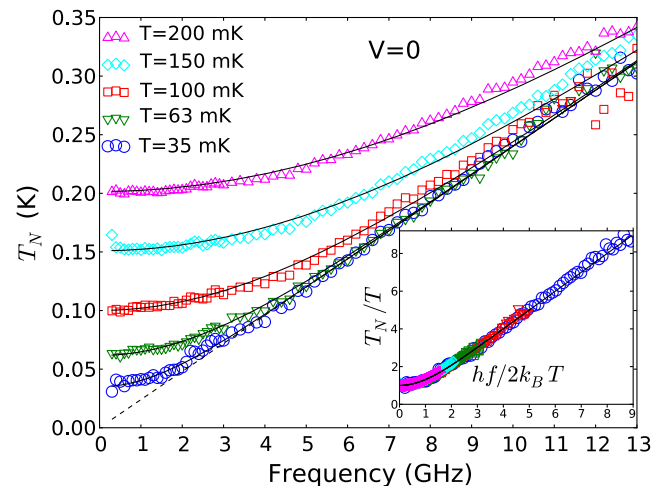


FIG. 2 (color online). Equilibrium noise temperature vs frequency for various electron temperatures T . Symbols are experimental data and solid lines are theoretical expectations of Eq. (2). Inset: Experimental rescaled noise temperature T_N/T vs rescaled frequency $hf/(2k_B T)$.

$$S_{\text{eq}}(f, T) = Ghf \coth\left(\frac{hf}{2k_B T}\right). \quad (2)$$

The black lines in Fig. 2 represent Eq. (2) with no adjustable parameter. Our data are in very good agreement with the theory. According to Eq. (2), the rescaled noise temperature T_N/T is a function of frequency and temperature only via the ratio $hf/(2k_B T)$. We show in the inset of Fig. 2 the measured T_N/T vs rescaled frequency $hf/(2k_B T)$ for all our data. We, indeed, observe that all the data collapse on a single curve for a wide interval of $hf/(2k_B T)$ between 0.075 and 9.

Shot noise spectroscopy.—Figure 3 shows the measurements of T_N vs frequency for various bias voltages V , at the lowest electron temperature $T = 35$ mK. At low frequencies $hf < eV$, one observes a plateau corresponding to the classical shot noise $S = eI$. When $hf \gg eV$, the vacuum fluctuations take over and $S = S_{\text{vac}}(f)$. Black lines in Fig. 3 are the theoretical predictions of the out-of-equilibrium noise spectral density [12]:

$$S(f, V, T) = \frac{1}{2} [S_{\text{eq}}(f_+, T) + S_{\text{eq}}(f_-, T)], \quad (3)$$

where $f_{\pm} = f \pm eV/h$. The data are in very good agreement with Eq. (3). Previous measurements of noise at few frequencies f have shown a kink at $V = hf/e$ in the voltage dependence of $S(V) - S(V = 0)$ or $\partial S/\partial V$ that is compatible with Eq. (3) [8,17,19–23]. Here, the full spectroscopy of the absolute spectral density is obtained, which is essential to deduce the current-current correlator in the time domain.

Current-current correlator in the time domain.—From the noise spectral density measured over a wide bandwidth, we calculate the current-current correlator in

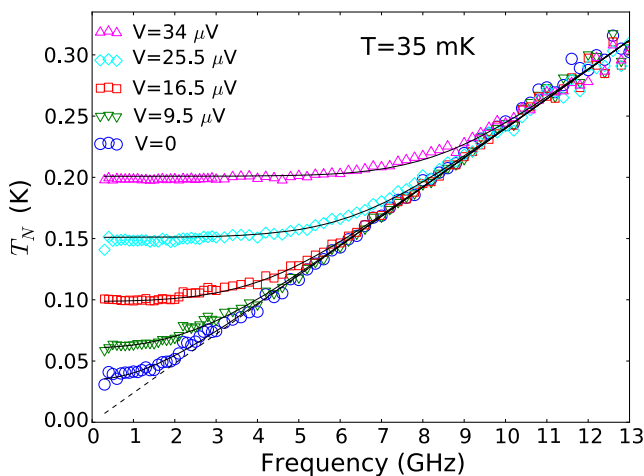


FIG. 3 (color online). Out-of-equilibrium noise temperature vs frequency for different dc voltage biases V at $T = 35$ mK. Symbols are experimental data and solid lines are theoretical expectations of Eq. (3).

the time domain by the Fourier transform (FT): $C(t) = \int_0^\infty (1/2\pi) \cos(2\pi ft) S(f) df$. Equation (3) leads to a very simple current-current correlator in the time domain: $C(t, T, V) = C_{\text{eq}}(t, T) \cos(eVt/\hbar)$. However, since $S_{\text{eq}}(f)$ diverges as $|f| \rightarrow \infty$, its FT is not well defined so that $C_{\text{eq}}(t, T)$ diverges at all times. To circumvent this problem, we define the *thermal excess noise* $\Delta S(f, T, V) = S(f, T, V) - S(f, T = 0, V)$ which goes to zero at high frequency and, thus, is well suited for FT. The corresponding current-current correlator should obey

$$\Delta C(t, T, V) = \Delta C_{\text{eq}}(t, T) \cos\left(\frac{eVt}{\hbar}\right), \quad (4)$$

where $\Delta C_{\text{eq}}(t, T) = C_{\text{eq}}(t, T) - C_{\text{eq}}(t, 0)$, and $C_{\text{eq}}(t, 0) = FT[S_{\text{vac}}(f)]$ corresponds to the (infinite) jitter associated with zero-point fluctuations. Note that in order to obtain such a simple and remarkable result, it is essential to subtract from $S(f, T, V)$ the noise spectral density at zero temperature but finite voltage, not $S_{\text{vac}}(f)$. $\Delta C_{\text{eq}}(t, T) = \Delta C(t, T = 35 \text{ mK}, V = 0)$ is obtained using $S_{\text{eq}}(f)$ of the inset of Fig. 2 using data collected at every temperature and the scaling law we have shown. To avoid artificial oscillations in the data due to FT within a finite frequency range, we have used a window at frequencies between 0.3 and 12 GHz. The result is plotted in Fig. 4 ($V = 0$, magenta symbols). Theoretical $\Delta C_{\text{eq}}(t, T)$ is plotted as a black line. We observe the thermal current-current fluctuations to decay with a time constant given by $\hbar/k_B T$ of ~ 100 ps for $T = 35$ mK.

Experimental data for the nonequilibrium correlator $\Delta C(t, T, V)$ at $T = 35$ mK are also shown in Fig. 4 for various voltages. One clearly observes that $\Delta C(t)$ oscillates

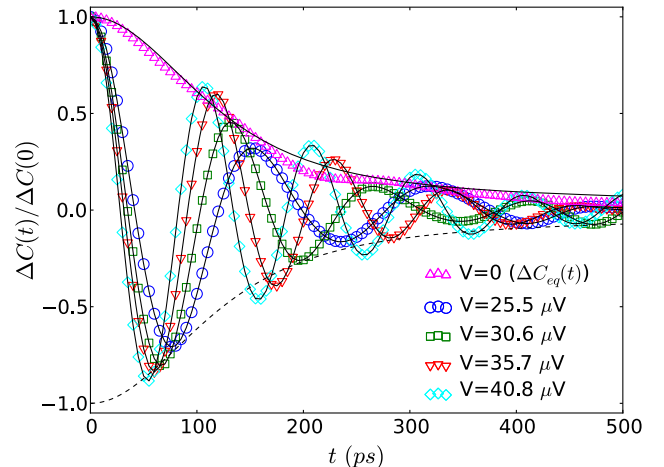


FIG. 4 (color online). Rescaled current-current correlator in the time domain for five different voltages at $T = 35$ mK. The data at $V = 0$ correspond to the correlator at equilibrium $\Delta C_{\text{eq}}(t, T)$. Its characteristic thermal decay time is given by $\hbar/k_B T \sim 100$ ps. Solid lines are theoretical expectations.

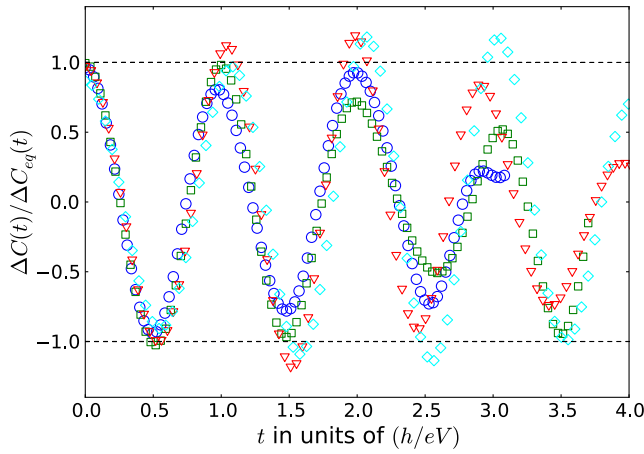


FIG. 5 (color online). Rescaled current-current correlator in the time domain vs reduced time eVt/h for various bias voltages $V = 25.5, 30.6, 35.7,$ and $40.8 \mu\text{V}$ (same symbols as Fig. 4).

within an envelope given by $\Delta C_{\text{eq}}(t)$, with a period that depends on the bias voltage. We show in Fig. 5 the experimental data for $\Delta C(t)/\Delta C_{\text{eq}}(t)$ as a function of the rescaled time h/eV . This rescaling clearly demonstrates the oscillation period being h/eV , in agreement with Eq. (4).

Another quantity of interest is the *voltage excess noise* introduced in Ref. [24]: $\Delta S_V(f, T, V) = S(f, T, V) - S(f, T, V = 0)$. The corresponding correlator in the time domain is $\Delta C_V(t, T, V) = -2C_{\text{eq}}(t, T)\sin^2(eVt/2\hbar)$. Both $\Delta C(t)$ and $\Delta C_V(t)$ oscillate with the same period h/eV , which is interpreted as an “electron coherence time” in Ref. [24]. Both $\Delta S(f)$ and $\Delta S_V(f)$ go to zero at high frequency and, thus, are experimentally accessible. However, $\Delta C_V(t)$ contains $C_{\text{eq}}(t)$, which diverges. The short time divergence of $C_{\text{eq}}(t)$ is, in theory, compensated by the sine squared. Experimentally, the finite bandwidth strongly affects oscillations in $\Delta C_V(t)$. Thus, while $\Delta C(t)$ and $\Delta C_V(t)$ contain the same information, the thermal excess noise is better suited to the experiment.

Interpretation.—These oscillations are the result of both the Pauli principle and Heisenberg uncertainty relation. To see this, let us consider a single channel conductor crossed at $t = 0$ by two electrons of energy E and E' . According to the Pauli principle, the energies must be different, $E \neq E'$. But how close can E and E' be? According to the Heisenberg uncertainty relation, it takes a time $t_H \approx \hbar/(|E - E'|)$ to resolve the two energies, so E and E' cannot be considered different for times shorter than t_H . Thus, if one electron crosses at time $t = 0$, the second one must wait. Since $|E - E'| < eV$, one has $t_H > h/eV$: there is a minimum time lag h/eV between successive electrons. The regular oscillations we observe on ΔC are a direct consequence of this blockade and reflect the fact that electrons try to cross the sample regularly at a pace of one electron per channel per spin direction every h/eV . A similar oscillation has been predicted to occur in the

distribution of the electrons’ waiting time [25]. The decay of $\Delta C(t)$ we observe at long time reflects the existence of a jitter which is of pure thermal origin.

At high bias voltage, $eV \gg k_B T, \hbar f$, the oscillation period h/eV becomes so small that the electrons no longer wait before tunneling. This is the classical limit, whose statistics is described by a Poisson distribution, with $S = eI$. At low bias voltage, there are correlations between successive tunneling electrons, and the resulting current distribution is no longer Poissonian.

Our measurements were made on a tunnel junction, a device in which all conduction channels have low transmission. In the general case, Eq. (4) is replaced by

$$\Delta C(t) = F\Delta C_{\text{eq}}(t) \cos\left(\frac{eVt}{\hbar}\right) + (1 - F)\Delta C_{\text{eq}}(t),$$

where F is the Fano factor. In the case of a perfect conductor, $F = 0$, and there is no oscillation of the current-current correlator, since there is no shot noise [4,5]. The tunnel junction, with $F = 1$, exhibits the largest oscillations of $\Delta C(t)$. Here the number of channels is irrelevant as long as channels are independent: the current-current correlator of the many channel sample is the sum of the single channel current-current correlators. This might, however, become questionable when interactions may lead, e.g., to correlations between channels.

In conclusion, our observations, by accessing time scales shorter than that relevant to quantum transport, have revealed how electrons behave when crossing a conductor at low temperature: they try to cross it at a regular pace h/eV , with a jitter $\hbar/k_B T$. This simple picture explains why and how current fluctuates, at least at the level of the second-order correlator. Higher-order correlators will require more experiments: for example, the third cumulant of current fluctuations has been predicted to be totally frequency independent, i.e., delta correlated in the time domain, for any temperature or voltage [26,27]. While this has been verified when one of the frequencies is greater than both eV/\hbar and $k_B T/\hbar$ [28], the question is still open when fully in the quantum regime.

We acknowledge fruitful discussions with W. Belzig and M. Aprili. We thank G. Laliberté for technical help. This work was supported by Grant No. ANR-11-JS04-006-01, the Canada Excellence Research Chairs program, the NSERC, the MDEIE, the FRQNT via the INTRIQ, the Université de Sherbrooke via the EPIQ, and the Canada Foundation for Innovation.

*Karl.Thibault@USherbrooke.ca

†Julien.Gabelli@U-PSud.fr

‡Christian.Lupien@USherbrooke.ca

§Bertrand.Reulet@USherbrooke.ca

[1] T. Martin and R. Landauer, *Phys. Rev. B* **45**, 1742 (1992).

- [2] M. Büttiker, *Phys. Rev. B* **46**, 12485 (1992).
- [3] G. B. Lesovik and L. S. Levitov, *Phys. Rev. Lett.* **72**, 538 (1994).
- [4] M. Reznikov, M. Heiblum, H. Shtrikman, and D. Mahalu, *Phys. Rev. Lett.* **75**, 3340 (1995).
- [5] A. Kumar, L. Saminadayar, D. C. Glatli, Y. Jin, and B. Etienne, *Phys. Rev. Lett.* **76**, 2778 (1996).
- [6] N. Ubbelohde, K. Roszak, F. Hohls, N. Maire, R. J. Haug, and T. Novotný, *Sci. Rep.* **2**, 374 (2012).
- [7] G. J. Dolan, *Appl. Phys. Lett.* **31**, 337 (1977).
- [8] R. J. Schoelkopf, P. J. Burke, A. A. Kozhevnikov, D. E. Prober, and M. J. Rooks, *Phys. Rev. Lett.* **78**, 3370 (1997).
- [9] W. Schottky, *Ann. Phys. (Berlin)* **362**, 541 (1918).
- [10] Some authors prefer to use the positive frequency representation for the noise spectral density and write Schottky's formula as $S = 2eI$. When the whole frequency range from $-\infty$ to ∞ is used, this formula takes the form $S = eI$. We have chosen the second form.
- [11] L. Spietz, K. W. Lehnert, I. Siddiqi, and R. J. Schoelkopf, *Science* **300**, 1929 (2003).
- [12] A. J. Dahm, A. Denenstien, D. N. Langenberg, W. H. Parker, D. Rogovin, and D. J. Scalapino, *Phys. Rev. Lett.* **22**, 1416 (1969).
- [13] Because of the very large bandwidth, the use of a circulator to prevent this effect was not possible. Insertion of cold attenuators might have lowered this effect but at the expense of a poorer signal-to-noise ratio and, thus, a longer averaging time.
- [14] J. B. Johnson, *Phys. Rev.* **32**, 97 (1928).
- [15] H. Nyquist, *Phys. Rev.* **32**, 110 (1928).
- [16] R. H. Koch, D. J. Van Harlingen, and J. Clarke, *Phys. Rev. Lett.* **47**, 1216 (1981).
- [17] J. Basset, H. Bouchiat, and R. Deblock, *Phys. Rev. Lett.* **105**, 166801 (2010).
- [18] H. B. Callen and T. A. Welton, *Phys. Rev.* **83**, 34 (1951).
- [19] J. Gabelli and B. Reulet, *J. Stat. Mech.* (2009) P01049.
- [20] E. Zakka-Bajjani, J. Ségala, F. Portier, P. Roche, D. C. Glatli, A. Cavanna, and Y. Jin, *Phys. Rev. Lett.* **99**, 236803 (2007).
- [21] E. Onac, F. Balestro, L. H. Willems van Beveren, U. Hartmann, Y. V. Nazarov, and L. P. Kouwenhoven, *Phys. Rev. Lett.* **96**, 176601 (2006).
- [22] S. Gustavsson, M. Studer, R. Leturcq, T. Ihn, K. Ensslin, D. C. Driscoll, and A. C. Gossard, *Phys. Rev. Lett.* **99**, 206804 (2007).
- [23] N. L. Schneider, G. Schull, and R. Berndt, *Phys. Rev. Lett.* **105**, 026601 (2010).
- [24] G. B. Lesovik, A. V. Lebedev, and G. Blatter, *Phys. Rev. B* **71**, 125313 (2005).
- [25] M. Albert, G. Haack, C. Flindt, and M. Büttiker, *Phys. Rev. Lett.* **108**, 186806 (2012).
- [26] D. S. Golubev, A. V. Galaktionov, and A. D. Zaikin, *Phys. Rev. B* **72**, 205417 (2005).
- [27] J. Salo, F. W. J. Hekking, and J. P. Pekola, *Phys. Rev. B* **74**, 125427 (2006).
- [28] J. Gabelli, L. Spietz, J. Aumentado, and B. Reulet, *New J. Phys.* **15**, 113045 (2013).